# Photoemission evidence for crossover from Peierls-like to Mott-like transition in highly strained VO_{2}

J. Laverock, A. R. H. Preston, D. Newby, Jr., K. E. Smith, S. Sallis, L. F. J. Piper, S. Kittiwatanakul, J. W. Lu, S. A. Wolf, M. Leandersson, and T. Balasubramanian

Phys. Rev. B **86**, 195124 — Published 16 November 2012

DOI: 10.1103/PhysRevB.86.195124

# Photoemission evidence for crossover from Peierls-like to Mott-like transition in highly strained $VO_2$

J. Laverock,[1] A. R. H. Preston,[1] D. Newby, Jr.,[1] K. E. Smith,[1] S. Sallis,[2] L. F. J. Piper,[2] S. Kittiwatanakul,[3] J. W. Lu,[4] S. A. Wolf,[3,4] M. Leandersson,[5] and T. Balasubramanian[5]

[1]*Department of Physics, Boston University, 590 Commonwealth Avenue, Boston, MA 02215, USA*
[2]*Department of Physics, Applied Physics and Astronomy, Binghamton University, Binghamton, NY 13902, USA*
[3]*Department of Physics, University of Virginia, Charlottesville, VA 22904, USA*
[4]*Department of Materials Science and Engineering, University of Virginia, Charlottesville, VA 22904, USA*
[5]*MAX-lab, Lund University, SE-221 00 Lund, Sweden*

We present a spectroscopic study that reveals that the metal-insulator transition of strained $VO_2$ thin films may be driven towards a purely electronic transition, which does not rely on the Peierls dimerization, by the application of mechanical strain. Comparison with a moderately strained system, which does involve the lattice, demonstrate the crossover from Peierls- to Mott-like transitions.

PACS numbers: 71.30.+h, 71.27.+a, 79.60.-i

The metal-insulator transition (MIT) in $VO_2$ is of both fundamental and technical interest, the former due to lingering important questions about its origins[1,2], and the latter due to possible applications in electronic devices such as ultrafast optical switches and field effect transistors[3,4]. In bulk $VO_2$, a large structural distortion accompanies the transition from the metallic rutile to the insulating monoclinic phase, which is known to impose a significant bottleneck on the timescale of the photo-induced transition[5]. Recently, the possibility of tailoring the transition temperature of the MIT in $VO_2$ through doping and/or nanoscale engineering[6,7,9] has heralded renewed interest in the potential application of $VO_2$ as a novel functional material. Whereas the mechanism of the MIT in bulk $VO_2$ is now reasonably well understood as an orbital-assisted collaborative Mott-Peierls transition (or associated variants)[10,11] (i.e. the MIT involves *both* the lattice and electron-correlation effects), the situation is less clear under large applied strain to the lattice. For example, the introduction of Nb as an isoelectronic dopant to V leads to an expansion of the $c/a$ constant, and eventually (for $\geq 15\%$ Nb) an insulating rutile phase is observed[12] (i.e. without any structural distortion).

The crucial aspects of the electronic structure of $VO_2$ center around the behavior of the V $a_{1g}$ orbital, which is oriented along the rutile $c$-axis ($c_R$-axis), and is also labelled as $d_{\|}$ for this reason. In the Peierls-type model, this orbital becomes split in the insulating monoclinic phase due to the dimerization of V atoms in the $c_R$-axis, and the associated twisting of the $VO_6$ octahedra pushes the $e_g^{\pi}$ bands upwards in energy, deoccupying them[1]. On the other hand, the correlation-driven mechanism[2] proposes that the strong correlations in the $a_{1g}$ orbital are screened by the $e_g^{\pi}$ band in the metallic phase. In the insulating phase, the $e_g^{\pi}$ states are empty, and the unscreened correlations open the gap. In the past, it has been difficult to distinguish between these two models, owing to the large structural distortion that accompanies the transition. However, a growing body of experimental and theoretical evidence supports that both are important in driving the MIT of bulk $VO_2$. For example, the local density approximation (LDA) fails to reproduce the MIT[13] without recourse to hybrid functionals beyond the LDA[14], and dynamical mean-field theory (DMFT) calculations[15,16] (that explicitly include dynamical electron correlations) are required to explain a good deal of the experimental data (for example, Refs. 6,10,12,17). We report here a photoemission spectroscopy (PES) study of strained $VO_2$ thin films, in which we show that the MIT may be driven towards a purely electronic transition, which does not rely on the

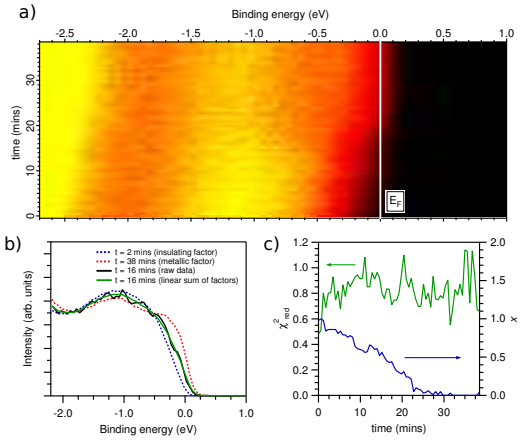


FIG. 1: V 3$d$ PES spectra of $VO_2$(110) during a heating cycle through the MIT. (a) A 2D map of the evolution of the V 3$d$ states with time. (b) Spectrum recorded half-way through the heating cycle compared with a linear sum of the insulating and metallic factors. (c) The goodness-of-fit parameter, $\chi^2$, between the time-dependent data and its fit to the two end-members of the series. Also shown is the evolution of the fraction, $x$, of the insulating spectrum used to describe the data.

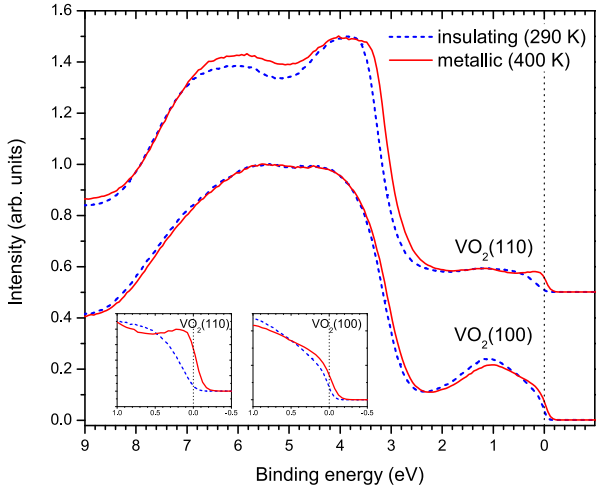


FIG. 2: PES spectra of the O $2p$ and V $3d$ states across the MIT of strained $VO_2$, recorded at 30 eV and with $E \parallel c_R$. The insets show an enlargement near $E_F$.

Peierls dimerization, by the application of mechanical strain.

High-quality thin films ($\sim 40$ nm) of $VO_2$ were grown on rutile $TiO_2$(110)- and $TiO_2$(100)-oriented substrates by reactive bias target ion-beam deposition[7]. X-ray diffraction measurements confirm the epitaxy of $VO_2$ with the substrate and establish the expanded $c_R$-axis lattice parameter of $VO_2$ compared with the bulk[8]. This tensive strain is found to be approximately twice as large for $VO_2/TiO_2(100)$ [hereafter referred to as $VO_2(100)$] at +3.7%, whereas the $c_R$-axis strain of $VO_2/TiO_2(110)$ [referred to as $VO_2(110)$] is +1.7%. Atomic force microscopy measurements[8] suggest a very low root-mean-square roughness of $\sim 0.3-0.4$ nm. Both samples display MITs above room temperature, at 345 K and 340 K for $VO_2(110)$ and $VO_2(100)$ respectively. Note that the MIT temperature of our $VO_2(110)$ film is lower than that observed in Ref. 6. PES measurements were carried out at beamline I3 (MAX III) of MAX-lab, Lund University, Sweden, using a Scienta R-4000 analyzer set to an energy resolution of 12 meV, with pressures in the analysis chamber of better than $5\times10^{-10}$ torr between room temperature and 150°C. The binding energy of the PES spectra were referenced to polycrystalline gold in electrical contact with the samples. The samples were prepared for ultra-high vaccuum measurements by several (one to three) repetitions of annealing in a partial $O_2$ environment ($\sim 450$°C, $1\times10^{-6}$ torr $O_2$, 30 mins). This procedure has been carefully developed to remove contaminant surface species from the samples without modifying the chemical environment of $VO_2$. Samples were aligned using low-energy electron diffraction and Laue x-ray diffraction. Soft x-ray spectroscopy measurements were performed at beamline X1B of the National Synchrotron Light Source (NSLS), Brookhaven. X-ray absorption spectroscopy (XAS) measurements were made in total electron yield mode with a beamline resolution of 0.2 eV, and the photon energy was calibrated with reference to $TiO_2$ spectra. Reonsant x-ray emission spectroscopy (RXES) measurements were recorded with a Nordgren-type grating spectrometer[18] set to an energy resolution of 0.7 eV and the instrument was calibrated using a Zn reference spectrum.

For *moderately-strained* $VO_2$(110), angle-integrated PES spectra of the V $3d$ states near $E_F$ are shown in Fig. 1a as a function of time during a slow heating cycle through the MIT. The evolution of the V $3d$ states are characterized by a transfer in spectral weight from $\sim 1$ eV binding energy towards $E_F$, associated with the shift in the quasiparticle peak energy that becomes gapped out below the MIT[15]. The small remnant weight near 1 eV in the metallic phase represents the lower Hubbard band (LHB) of the rutile metallic phase, and is slightly shifted towards higher binding energies, in agreement with cluster DMFT (cDMFT) results[15]. These results are in excellent agreement with previous PES measurements of both bulk and thin-film $VO_2$[17,19,20]. In Fig. 1b, a comparison of the metallic and insulating spectra (end members of the heating cycle) is made with a spectrum recorded midway through the series. A linear superposition of the two end members is also shown, supporting real space measurements of bulk $VO_2$ that find no evidence of an intermediate phase in the transition[21]. Indeed, the spectra throughout the heating cycle have been carefully analysed using a factor analysis approach, and we find only two factors are required to reproduce the spectra for all energies and temperatures measured (Fig. 1c).

In Fig. 2, angle-integrated PES spectra of the O $2p$ and V $3d$ states of moderately strained $VO_2$(110) and $VO_2$(100) are shown across the MIT. In $VO_2$(110), a large gap develops in the insulating (room temperature) spectra, the magnitude of which is $\sim 300$ meV (measured from extrema in the first derivative). However, for the *highly strained* $VO_2$(100) system (Fig. 2b), the magnitude of the insulating gap is much smaller, at $\lesssim 50$ meV, with only a weak shift in the O $2p$ band. Here, the strong double-peaked structure in the O $2p$ manifold is less prominent; rather the spectra exhibit broad, asymmetric peaks, similar to earlier PES studies of $VO_2$[19]. The weak opening of the insulating gap in films under high strain compared to moderate strain constitutes our first clue that the physics of the MIT may be different for highly strained $VO_2$(100).

In order to understand in more detail the behavior of the two systems across the MIT, we now focus on the dependence of the V $3d$ states with photon polarization. By rotating the polarization vector of the incident photons, it is possible to couple to different symmetry orbitals, providing orbital-resolution to PES measurements. In particular, for $E \parallel c_R$, the matrix elements that couple the PES process of the V $3d$ states are maximized for the $a_{1g}$ states. In Fig. 3a, high-resolution angle-integrated spectra above and below the MIT are shown for $E \parallel c_R$ and $E \perp c_R$ for $VO_2$(110), normalized to the intensity between 1.0 and 1.2 eV. It is clear from Fig. 3a that

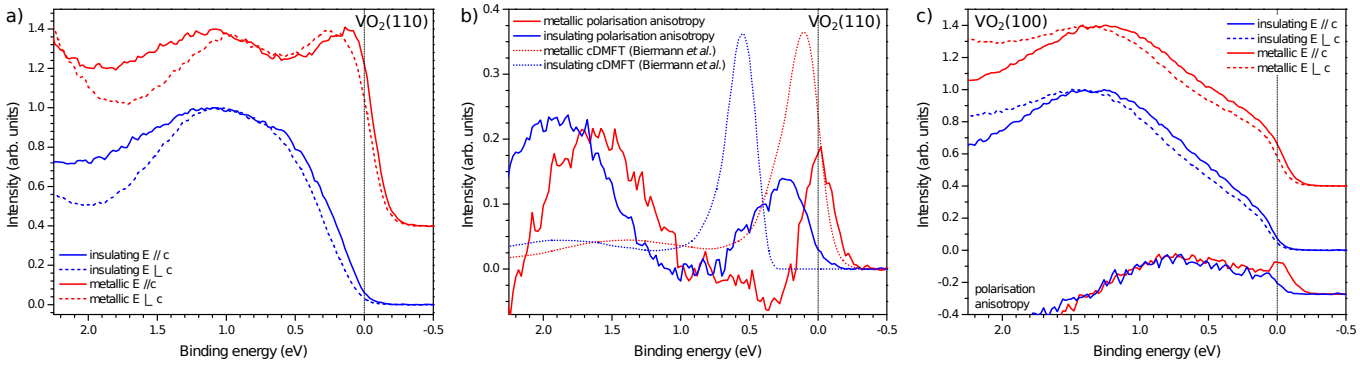


FIG. 3: High resolution V 3*d* PES spectra across the MIT of the $VO_2$ thin films at 30 eV. (a) Spectra of moderately-strained $VO_2$(110) for two different incident photon polarizations: $E \parallel c_R$ and $E \perp c_R$. (b) Polarization anisotropy of $VO_2$(110) in the insulating and metallic phases compared with cDMFT calculations of Biermann *et al.*[15]. (c) Polarization-dependent spectra of highly-strained $VO_2$(100). Shown at the bottom of the figure is the weak polarization anisotropy for this system.

there is a substantial change in the shape of the spectra across the transition, and even in the relative energies of features between different polarizations. In Fig. 3b, the polarization anisotropy, $I_\parallel - I_\perp$, is shown for the spectra from metallic and insulating phases, representing approximate experimental PES spectra of the $a_{1g}$ orbital. In the metallic phase, the quasiparticle peak is centered at $E_F$, with the LHB at $\sim 1.5$ eV. The quasiparticle peak shifts down to $\sim 0.4$ eV in the insulating spectra, accompanied by a shift of the LHB to $\sim 1.8$ eV. These results are in remarkable agreement with the cDMFT calculations of the $a_{1g}$ orbital of Biermann *et al.*[15], which are reproduced by the dotted lines in Fig. 3b. In the $M_1$ insulating phase of $VO_2$, the $a_{1g}$ state is overwhelmingly the most occupied of the V $t_{2g}$ orbitals (contributing $\sim 80\%$ to the total occupied density of states), whereas these orbitals are almost evenly populated in the metallic rutile phase. Further evidence of this interpretation is provided by parameter-free analysis of the insulating spectra. For $E \perp c_R$, the extremum of the first derivative is located $\sim 300$ meV below $E_F$, but is much smaller for $E \parallel c_R$ at $\sim 150$ meV (the associated error in determining this quantity is $\sim 10$ meV), supporting the cDMFT results that show the $a_{1g}$ orbital lies closer to $E_F$ than the $e_g^\pi$ states.

In Fig. 3c, high-resolution spectra of highly-strained $VO_2$(100) are shown alongside their polarization anisotropy. These spectra show much weaker anisotropy, with very similar shapes both above and below the transition: a very small quasiparticle 'peak' shifts to deeper energies (and diminishes in intensity) in the insulating phase. Examination of the first derivative of both photon polarizations in the insulating phase reveal both extrema lie $\sim 50$ meV below $E_F$, demonstrating the relative isotropy of the gap for $VO_2$(100). The similarity of the polarization anisotropy across the MIT suggests that the population of orbitals is approximately the same in the insulating and metallic phases, inconsistent with the structural distortion that preferentially occupies the $a_{1g}$ orbitals. DMFT calculations of the rutile phase with varying on-site Hubbard $U$ have demonstrated that an *insulating rutile* phase (i.e. without structural distortion) may be stabilized for large values of $U$[16]. Bulk rutile $VO_2$ is believed to lie close to (but on the metallic side of) the crossover region (in which both metallic and insulating phases are stable). However, the nature of the insulating rutile phase is very different from the insulating $M_1$ phase of bulk $VO_2$, and is characterized by a very small insulating gap and almost even population of $t_{2g}$ orbitals (similar to the metallic phase). Our PES measurements of highly strained $VO_2$(100) are consistent with such a scenario, in which we observe both a very small insulating gap ($\lesssim 50$ meV) *and* similar populations of the $t_{2g}$ orbitals across the transition, in contrast to our results of the moderately strained $VO_2$(110) system. It is suggested that the large tensive strain of $VO_2$(100) leads to a narrowing of the bandwidth, $W$, of the $t_{2g}$ bands, and the accompanying increase in the relative importance of electron correlations, characterized by $U/W$. In this simple model (schematically depicted in Fig. 4), $U/W_{bulk} < U/W_{(110)} < U/W_{(100)}$, and the system may be pushed into the coexistence region of the phase diagram, with a crossover from the traditional lattice-electronic mechanism of the bulk system to an electronic one for the highly strained system. For Nb-doped $VO_2$, an insulating rutile phase has already been observed, for which the mechanism was interpreted as electronic in origin, assisted by the disorder[12]. Here, we show that such an electronic driven transition can also be stabilized for pure $VO_2$ at ambient pressures, by introducing large tensive strain to the system. These findings are in agreement with a recent optical study of similar $VO_2$ thin films, in which the decoupling of the structural and electronic components of the MIT was reported[22]. One can then circumvent the well-known structural bottleneck in the timescale of the transition[5], of substantial value for applications that are envisaged to exploit the ultra-fast nature of the MIT of $VO_2$[3,23]. Furthermore, this observation that the electronic-driven transition in highly-strained $VO_2$ is quite different to that in moder-

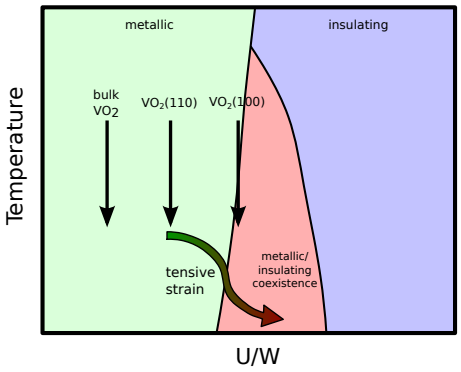


FIG. 4: Schematic representation of the impact of tensive $c_R$-axis strain on the phase diagram of $VO_2$. Tensive strain expands the $c_R$-axis, narrowing the bandwidth, $W$, and leading to an increase in the relative importance of electron correlations, $U/W$. The phase diagram is based on the DMFT results of Ref. 16.

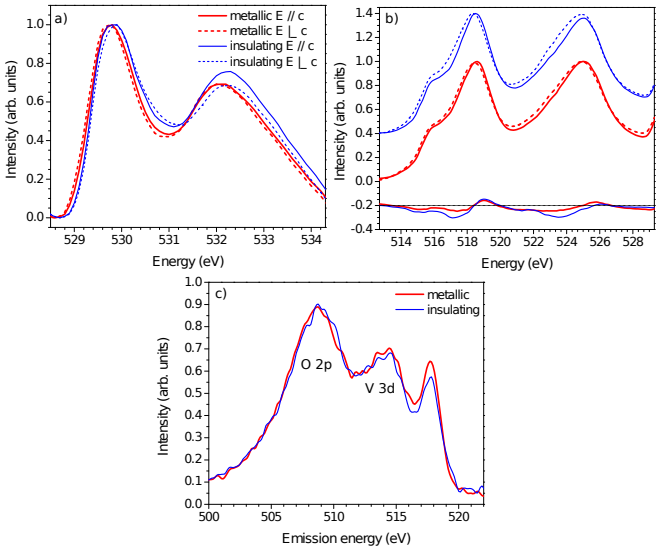


FIG. 5: Soft x-ray measurements on $VO_2$(100) through the MIT. (a) Polarization-dependent O $K$-edge XAS. (b) Polarization-dependent V $L_{3,2}$-edge XAS. At the bottom of the figure, the anisotropy between $E \parallel c_R$ and $E \perp c_R$ are shown. (c) RXES spectra, recorded at the V $L_3$-edge peak.

ately strained $VO_2$ (in agreement with DMFT) supplies additional weight to the argument that *both* the Peierls-type and Mott-type mechnisms are important in stabilising the $M_1$ phase of bulk $VO_2$.

In order to reinforce our PES results, soft x-ray XAS and RXES measurements have also been performed, and are shown in Fig. 5. It is well known that XAS of the O $K$-edge[17,24] and V $L_{3,2}$-edge[10] are sensitive to changes in the population of the $t_{2g}$ orbitals across the MIT, and we have previously demonstrated that RXES at the V $L_3$-edge is a sensitive probe of the structural distortion associated with the MIT in moderately strained $VO_2$[25,26]. For $VO_2$(100), we find our XAS spectra from films in the metallic phase at the V $L_{3,2}$- and O $K$-edges (Fig. 5a,b) are in good agreement with other such measurements of the metallic phase of bulk and moderately-strained $VO_2$[10,17,25]. However, the spectra from insulating films are almost identical to those from the metallic films, with only a weak shift in the O $K$-edge threshold (of $\lesssim 0.1$ eV, which is the accuracy of these measurements) indicating the very small insulating gap. In particular, the $a_{1g}$ ($d_\parallel$) peak, a signature of V-V dimerization in the distorted monoclinic phase, is absent at low temperature. Similarly, RXES measurements of $VO_2$(100) are not found to exhibit any temperature dependence across the MIT (Fig. 5c). For moderately strained $VO_2$(110), a large change in the relative intensity of the V $3d$ feature at $\sim$ 515 eV is related to the different bonding environments of V-O induced by the structural distortion of the $VO_6$ octahedra at the MIT[25]. Here, we find this ratio is the same for the insulating and metallic spectra of $VO_2$(100), indicating the twisting of the $VO_6$ octahedra is absent in this sample. Both of these observations are consistent with the PES evidence described above, and together suggest a rutile-like structure exists in both metallic and insulating phases. Moreover, recent temperature-dependent x-ray diffraction measurements on similar thin films[22] suggest that the change in lattice spacing at the MIT is very weak (by an order of magnitude) for their highly strained $VO_2$(100) films compared with the bulk, and is decoupled from the electronic transition. For our $VO_2$(100) samples, we find a similar suppression of the lattice spacing component of the transition compared with $VO_2$(110)[8], emphasizing the weaker role of the lattice in the MIT of $VO_2$(100).

In summary, we have observed a crossover from a Mott-Peierls-like transition to a Mott-like transition with an increase in tensive strain along the $c_R$-axis in $VO_2$ through several different spectroscopic techniques. XAS and RXES were used to demonstrate the absence of the large structural distortion at the MIT that characterize bulk and moderately strained $VO_2$. PES measurements revealed a weak insulating gap as well as the suppression of orbital redistribution across the transition. We further showed that by exploiting the relative polarization of the incident photons, PES can probe changes in the orbital occupation across electronic phase transitions. Our observations have important implications for novel functional material engineering of $VO_2$, suggesting a route towards circumventing the structural bottleneck in the ultrafast timescale of the MIT.

**Acknowledgements**. The authors acknowledge useful discussions with R. D. Averitt, E. Abreu and M. Liu. The Boston University program is supported in part by the Department of Energy under Grant No. DE-FG02-98ER45680. The NSLS, Brookhaven, is supported by the U.S. Department of Energy under Contract No. DE-AC02-98CH10886. SK, JWL, SAW are thankful to the financial support from the Army Research Office through MURI grant No. W911-NF-09-1-0398.

[1] J. B. Goodenough and H. Y.-P. Hong, Phys. Rev. B **8**, 1323 (1973).
[2] A. Zylbersztejn and N. F. Mott, Phys. Rev. B **11** 4383 (1975).
[3] M. Rini, A. Cavalleri, R. W. Schoenlein, R. López, L. C. Feldman, R. F. Haglund, Jr., L. A. Boatner and T. E. Haynes, Optics Lett. **30**, 558 (2005).
[4] H.-T. Kim, B.-G. Chae, D.-H. Youn, S.-L. Maeng, G. Kim, K.-Y. Kang and Y.-S. Lim, New J. Phys. **6**, 52 (2004).
[5] A. Cavalleri, Th. Dekorsy, H. H. W. Chong, J. C. Kieffer and R. W. Schoenlein, Phys. Rev. B **70**, 161102(R) (2004).
[6] Y. Muraoka and Z. Hiroi, Appl. Phys. Lett. **80**, 583 (2002).
[7] K. G. West, J. W. Lu, J. Yu, D. Kirkwood, W. Chen, Y. H. Pei, J. Claassen and S. A. Wolf, J. Vac. Sci. Technol. A **26**, 133 (2008).
[8] See Supplemental Material at [url] for details of the sample growth and characterization.
[9] J. Cao, E. Ertekin, V. Srinivasan, W. Fan, S. Huang, H. Zheng, J. W. L. Yim, D. R. Khanal, D. F. Ogletree, J. C. Grossman and J. Wu, Nature Nanotech. **4**, 732 (2009); J. Cao, Y. Gu, W. Fan, L. Q. Chen, D. F. Ogletree, K. Chen, N. Tamura, M. Kunz, C. Barrett, J. Seidel and J. Wu, Nano Lett. **10**, 2667 (2010).
[10] M. W. Haverkort, Z. Hu, A. Tanaka, W. Reichelt, S. V. Streltsov, M. A. Korotin, V. I. Anisimov, H. H. Hsieh, H.-J. Lin, C. T. Chen, D. I. Khomskii and L. H. Tjeng, Phys. Rev. Lett. **95**, 196404 (2005).
[11] C. Weber, D. D. O'Regan, N. D. M. Hine, M. C. Payne, G. Kotliar and P. B. Littlewood, arXiv:1202.1423v1 (2012).
[12] P. Lederer, H. Launois, J. P. Pouget, A. Casalot and G. Villeneuve, J. Phys. Chem. Solids **33**, 1969 (1972).
[13] V. Eyert, Ann. Phys. (Leipzig) **11**, 650 (2002).
[14] V. Eyert, Phys. Rev. Lett. **107**, 016401 (2011).
[15] S. Biermann, A. Poteryaev, A. I. Lichtenstein and A. Georges, Phys. Rev. Lett. **94**, 026404 (2005).
[16] B. Lazarovits, K. Kim, K. Haule and G. Kotliar, Phys. Rev. B **81**, 115117 (2010).
[17] T. C. Koethe, Z. Hu, M. W. Haverkort, C. Schüßler-Langeheine, F. Venturini, N. B. Brookes, O. Tjernberg, W. Reichelt, H. H. Hsieh, H.-J. Lin, C. T. Chen and L. H. Tjeng, Phys. Rev. Lett. **97**, 116402 (2006).
[18] J. Nordgren, G. Bray, S. Cramm, R. Nyholm, J.-E. Rubensson and N. Wassdahl, Rev. Sci. Instrum. **60**, 1690 (1989).
[19] K. Okazaki, H. Wadati, A. Fujimori, M. Onoda, Y. Muraoka and Z. Hiroi, Phys. Rev. B **69**, 165104 (2004) K. Saeki, T. Wakita, Y. Muraoka, M. Hirai, T. Yokoya, R. Eguchi and S. Shin, Phys. Rev. B **80**, 125406 (2009).
[20] R. Eguchi, M. Taguchi, M. Matsunami, K. Horiba, K. Yamamoto, Y. Ishida, A. Chainani, Y. Takata, M. Yabashi, D. Miwa, Y. Nishino, K. Tamasaku, T. Ishikawa, Y. Senba, H. Ohashi, Y. Muraoka, Z. Hiroi and S. Shin, Phys. Rev. B **78**, 075115 (2008); T. Kanki, H. Takami, S. Ueda, A. N. Hattori, K. Hattori, H. Daimon, K. Kobayashi and H. Tanaka, Phys. Rev. B **84**, 085107 (2011).
[21] S. A. Corr, D. P. Shoemaker, B. C. Melot and R. Seshadri, Phys. Rev. Lett. **105**, 056404 (2010).
[22] E. Abreu, M. Liu, J. Lu, K. G. West, S. Kittiwatanakul, W. Yin, S. A. Wolf and R. D. Averitt, arXiv:1112.1573v1 (2011).
[23] A. Cavalleri, Cs. Tóth, C. W. Siders, J. A. Squier, F. Ráksi, P. Forget and J. C. Kieffer, Phys. Rev. Lett. **87**, 237401 (2001).
[24] M. Abbate, F. M. F. de Groot, J. C. Fuggle, Y. J. Ma, C. T. Chen, F. Sette, A. Fujimori, Y. Ueda and K. Kosuge, Phys. Rev. B **43**, 7263 (1991).
[25] J. Laverock, L. F. J. Piper, A. R. H. Preston, B. Chen, J. McNulty, K. E. Smith, S. Kittiwatanakul, J. W. Lu, S. A. Wolf, P.-A. Glans and J.-H. Guo, Phys. Rev. B **85**, 081104(R) (2012).
[26] L. F. J. Piper, A. DeMasi, S. W. Cho, A. R. H. Preston, J. Laverock, K. E. Smith, K. G. West, J. W. Lu and S. A. Wolf, Phys. Rev. B **82**, 235103 (2010).